

# Ionic Chemistry of Tetravinylsilane Cation (TVS<sup>+</sup>) Formed by Electron Impact: Theory and Experiment

V. Brites, G. Chambaud, and M. Hochlaf\*

Laboratoire Modélisation et Simulation Multi Echelle, MSME FRE 3160 CNRS, Université Paris-Est, 5 bd Descartes, 77454 Marne-la-Vallée, France

J. Kočíšek, J. L. Cayao Diaz, and Š. Matejíček

Department of Experimental Physics, Faculty of Mathematics, Physics and Informatics, Comenius University in Bratislava, Mlynská dolina, SK-842 48 Bratislava, Slovakia

F. Krčma

Faculty of Chemistry, Brno University of Technology, Purkyňova 118, CZ-612 00 Brno, Czech Republic

Received: March 4, 2009; Revised Manuscript Received: April 22, 2009

We performed experimental and ab initio studies on tetravinylsilane cation (TVS<sup>+</sup>) and its ionic and neutral fragmentation products. The aim of the study is the assignment of the products formed in electron impact ionization reaction of TVS. The experimental data were compared with ab initio data calculated at the MP2/cc-pVDZ level of theory. We found good agreement between the calculated reaction enthalpies and experimental appearance energies of the ions. More generally, our calculations reveal that there is a competition between intramolecular isomerization and fragmentation processes occurring after ionization of TVS, leading to the formation of a multitude of neutral and ionic species important for characterizing the silicon–carbon-containing plasma and media. New routes for the synthesis of bearing silicon molecules are suggested.

## I. Introduction

In 1985, Raabe and Michl<sup>1</sup> showed the rich chemistry of organosilicon compounds. For the gaseous silicon-containing cations, the combined theoretical and experimental investigations of Apeloig et al.<sup>2</sup> pointed out the complex processes taking place after their formations by electron ionization. This includes intramolecular rearrangement phenomena together with unimolecular decompositions. Later on, Magnera et al. confirmed once more these findings by studying the laser ablation of a variety of polysilanes at 308 nm.<sup>3</sup> More generally, this rich chemistry, either neutral or ionic, produces a wide variety of molecular species of importance for organic chemistry,<sup>4,5</sup> astrophysics,<sup>6,7</sup> and plasma physical chemistry.<sup>8,9</sup>

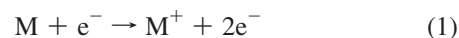
We are interested here in the chemistry of the tetravinylsilane cation (TVS<sup>+</sup>) and its derived silicon-bearing fragments. The neutral TVS was widely studied by means of IR and Raman spectroscopies<sup>10</sup> and gas-phase electron diffraction technique.<sup>11</sup> Similar to the other organosilicon compounds, the laser-induced photolysis<sup>12</sup> and the multiphoton IR-induced decomposition studies<sup>13</sup> reveal the formation of several molecular species. Hence, a complex gas-phase chemistry is taking place either in the ground or in the electronic excited states of TVS. Finally, the ionization energy of TVS was deduced from the earlier photoelectron spectrum of Schweig et al.<sup>14</sup> In contrast, nothing is available in the literature concerning the TVS<sup>+</sup> ion despite its importance, at least on plasma physics. Indeed, TVS<sup>+</sup> is suspected to be present and involved during the formation of TVS polymer films.<sup>15–17</sup> These experimental works suggest also the occurrence of isomerization processes under these conditions,

resulting in functional multilayer organosilicon surfaces with new physicochemical properties and therefore important industrial applications.

This work presents a combined experimental and theoretical investigation, where the TVS<sup>+</sup> is formed after electron impact ionization of the corresponding neutral molecule. The theoretical data are deduced from large ab initio calculations on the structural parameters and energy diagram of TVS<sup>+</sup> and connected ions and neutral fragments. Close comparison between our theoretical and experimental data allows attribution of the mass spectrometric spectra and the identification of the unimolecular reaction pathways undertaken by the TVS<sup>+</sup> cation hence formed.

## II. Methodologies

**1. Experimental Setup.** The electron impact ionization reaction is described by the equation



The molecular ion (M<sup>+</sup>) either can be formed as a stable species or may dissociate or rearrange. The present experiment was carried out using crossed electron/molecule beam apparatus in the Bratislava laboratory. This apparatus has been described in detail previously.<sup>18</sup> Thus, only a brief description is given here. A schematic view of the apparatus is shown in Figure 1. The electron beam is formed in a trochoidal electron monochromator with an electron energy resolution in the present experiment of about 140 meV. The calibration of the electron energy scale is performed by measurement of the Ar<sup>+</sup> ion

\* To whom correspondence should be addressed. E-mail: hochlaf@univ-mlv.fr.

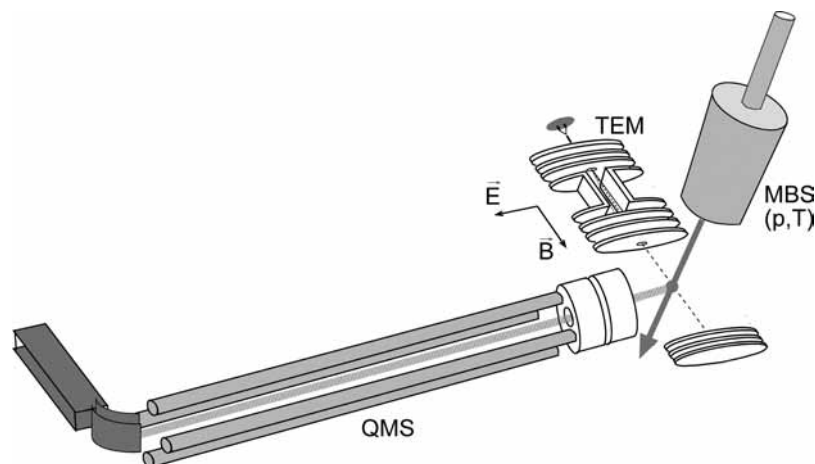


**Figure 1.** Schematic view of the apparatus.

efficiency curve for the reaction  $e^- + \text{Ar} \rightarrow \text{Ar}^+ + 2e^-$  that has an established value of ionization energy of  $15.759 \pm 0.001$  eV.<sup>19</sup>

The molecular beam is produced in a temperature-controlled effusive molecular beam source. The beam is formed via effusion of gas-phase TVS through a capillary (0.5-mm diameter and 4-mm long) and an external aperture. The ions formed in the intersection between the electron and the molecular beam are extracted into a quadrupole mass spectrometer. The mass spectrometrically analyzed ion signal is recorded as a function of the electron energy. The measured signal is accumulated to achieve high sensitivity and accuracy and to detect reactions with very low cross sections. The measured ionization efficiency curves are analyzed using the data analysis described in our previous article devoted to the measurement of appearance energies.<sup>18</sup> This method takes into account the finite width of the kinetic energy distribution function of the electrons in the electron beam and enables the determination of appearance energies of the ions with high accuracy. The thresholds are determined by linear extrapolations.

**2. Computations.** To establish a methodology for accurate treatment of  $\text{TVS}^+$ , its isomers, and fragmentation products, different computational methods were applied and tested. They include density functional theory and post Hartree–Fock techniques, such as Moller–Plesset (MP2) and coupled clusters approaches. Several basis sets were also tested (such as STO-3G, cc-pVDZ, cc-pVTZ).<sup>20,21</sup> Our calculations on the neutral TVS show that we obtain data accurate enough and comparable directly to the experimental results (i.e., equilibrium geometry, vibrational, and rotational constants) at the MP2/cc-pVDZ level of theory with reasonable computation cost. Therefore, the electronic structure calculations of all species discussed below were performed at the MP2 level of theory<sup>22,23</sup> and where the complete cc-pVDZ basis set of Dunning and co-workers was employed for the description of the Si, C, and H atoms.<sup>20,21</sup> This results in 190 contracted Gaussian functions to be treated. All electronic calculations were done using the Molpro program suite.<sup>24</sup> Our calculated energies were predicted to be accurate to 0.2–0.3 eV.

For the molecular species of interest here, harmonic frequencies were determined at the MP2/cc-pVDZ level using the standard options implemented in the Molpro package. The results of the frequency calculations will be published separately.<sup>25</sup>

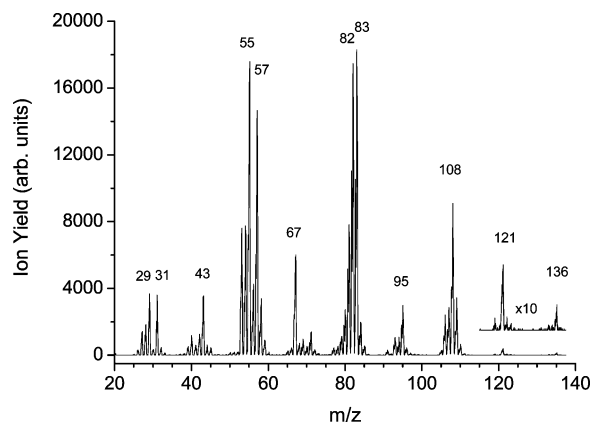


**Figure 2.** Mass spectrum of tetravinylsilane at the incident energy of electrons of 70 eV.

### III. Results

**1. Mass Spectrum of TVS.** Figure 2 displays a typical mass spectrum of TVS obtained for incident electron energy of 70 eV. A multitude of peaks are observed in this spectrum corresponding to mass/charge ratios of 136, 121, 108, 95, 83, 82, 67, 57, 55, 43, 31, and 29 (all values are in amu). Under these experimental conditions, the mass spectrum is dominated by the singly charged ions; the multiply charged ions contribution is very limited. The 136 peak corresponds to the parent  $\text{TVS}^+$  ion or to its isomers (see below). The assignment of the peaks at 109, 82, 55, and 28 amu is straightforward, a priori, because they may correspond to the trivial decomposition of  $\text{TVS}^+$  by losing one vinyl group. Nevertheless, some of the peaks, for instance at 83 and 57, cannot be attributed to direct cleavage of the C–Si bonds, and thus complex rearrangement of the products after ionization has to be taken into account. Finally, Table 1 gives the relative intensities of the ion peaks in the mass spectrum depicted in Figure 2. The parent peak (at 136 amu) has only very weak intensity, which indicates that the  $\text{TVS}^+$  ion is subjected to complex chemistry populating the daughter peaks. Moreover, we see a difference between present mass spectrum and the standard TOF spectrum at NIST.<sup>19</sup> We notice clear differences for the most abundant peak at mass 83 and also a significant difference at masses  $\sim 55$  and 108. This is, here again, a signature of higher dissociation rates in our experiment during the flight time of ions before reaching the ion detector.

Table 1 lists the measured appearance energies (AE) derived from the present experiment. Except for the AE( $\text{TVS}^+$ ), all other

**TABLE 1: Positive Ions, Their Masses, Relative Intensity, and Appearance Energies Estimated from Experiment<sup>a</sup>**

| mass (amu) | tentative assignment  | computed AE (eV) | measured AE (eV) | relative intensity (au) |
|------------|---|------------------|------------------|-------------------------|
| 29         | SiH <sup>+</sup>  | <sup>b</sup>     | 13               | 15.6                    |
| 31         | SiH <sub>3</sub> <sup>+</sup>   | <sup>b</sup>     | 13               | 13.8                    |
| 43         | CH <sub>3</sub> Si <sup>+</sup> , C <sub>3</sub> H <sub>7</sub> <sup>+</sup>        | <sup>b</sup>     | 11               | 15.9                    |
| 55         | [55A <sup>+</sup> ] + [81A]   | 9.6              | two thresholds:  | 86.7                    |
|            | [55B <sup>+</sup> ] + [81A]   | 10.3             | 12.3             |                         |
|            | [55C <sup>+</sup> ] + [81A]   | 9.1              | 13.4             |                         |
|            | [55D <sup>+</sup> ] + C <sub>4</sub> H <sub>6</sub> + C <sub>2</sub> H <sub>3</sub> | 12.4             |                  |                         |
|            | [55D <sup>+</sup> ] + [81B]   | 9.7              |                  |                         |
| 57         | [57A <sup>+</sup> ] + [79A]   | 13.0             | 9.5              | 80.0                    |
|            | [57A <sup>+</sup> ] + [79B]   | 8.8              |                  |                         |
|            | [57B <sup>+</sup> ] + [79C]   | 12.4             |                  |                         |
|            | [57C <sup>+</sup> ] + [79C]   | 10.9             |                  |                         |
| 67         | [67 <sup>+</sup> ] + [69]   | 10.6             | 12               | 35.5                    |
| 82         | [82 <sup>+</sup> ] + 2 C <sub>2</sub> H <sub>3</sub>                                | 14.8             | 9.6              | 97.6                    |
|            | [82 <sup>+</sup> ] + C <sub>4</sub> H <sub>6</sub>                                  | 9.4              |                  |                         |
| 83         | [83 <sup>+</sup> ] + C <sub>2</sub> H <sub>3</sub> + C <sub>2</sub> H <sub>2</sub>  | 12.4             | 9.8              | 100.0                   |
|            | [83 <sup>+</sup> ] + C <sub>4</sub> H <sub>5</sub>                                  | 9.8              |                  |                         |
| 95         | [95A <sup>+</sup> ] + [41A]   | 12.9             | 9.7              | 15.6                    |
|            | [95A <sup>+</sup> ] + [41B]   | 14.3             |                  |                         |
|            | [95B <sup>+</sup> ] + [41A]   | 8.2              |                  |                         |
|            | [95B <sup>+</sup> ] + [41B]   | 9.6              |                  |                         |
|            | [95C <sup>+</sup> ] + [41A]   | 8.0              |                  |                         |
|            | [95C <sup>+</sup> ] + [41B]   | 9.4              |                  |                         |
| 108        | [108A <sup>+</sup> ] + C <sub>2</sub> H <sub>4</sub>                                | 11.1             | 9.4              | 53.4                    |
|            | [108B <sup>+</sup> ] + C <sub>2</sub> H <sub>4</sub>                                | 9.8              |                  |                         |
|            | [108C <sup>+</sup> ] + C <sub>2</sub> H <sub>4</sub>                                | 9.5              |                  |                         |
|            | [108D <sup>+</sup> ] + C <sub>2</sub> H <sub>4</sub>                                | 7.8              |                  |                         |
| 109        | [109 <sup>+</sup> ] + C <sub>2</sub> H <sub>3</sub>                                 | 10.0             | 9.4              | 18.0                    |
| 121        | [121A <sup>+</sup> ] + CH <sub>3</sub>  | 16.5             | 10.1             | 3.4                     |
|            | [121B <sup>+</sup> ] + CH <sub>3</sub>  | 10.7             |                  |                         |
|            | [121C <sup>+</sup> ] + CH <sub>3</sub>  | 9.2              |                  |                         |
|            | [121D <sup>+</sup> ] + CH <sub>3</sub>  | 7.9              |                  |                         |
|            | [121E <sup>+</sup> ] + CH <sub>3</sub>  | 6.8              |                  |                         |
| 136        | [TVS <sup>+</sup> ]   | 9.45             | 9.5              | 1.2                     |
|            | [136 <sup>+</sup> ]   | 9.07             |                  |                         |
|            | [DMPS <sup>+</sup> ]  | 5.7              |                  |                         |

<sup>a</sup> We also quote the calculated appearance energies and our tentative assignment of these reaction channels (see text for more details). The energies are given with respect to the neutral TVS equilibrium structure. Readers are referred to Figure 3 for the designation of the molecular species. <sup>b</sup> Numerous neutral counter partner structures are possible.

quantities are new. The appearance energy for the parent peak ( $m/z = 136$ ) corresponds also to the ionization energy (IE) of TVS. Our measured IE is  $9.5 \pm 0.12$  eV, which is consistent with our computed MP2/cc-pVDZ vertical ionization energy of 9.45 eV. These values are in good agreement with the ionization energy of 9.3 eV obtained by Schweig et al.<sup>14</sup>

**2. Theoretical Results.** Table 1 and Figure 3 present the main theoretical data obtained from our study of TVS<sup>+</sup>, isomers, and their neutral and positively charged fragments. These data correspond to structures identified here and their appearance energies computed at the MP2/cc-pVDZ level of theory. These energies are given with respect to the TVS equilibrium energy without considering the zero point vibrational energy corrections. For simplicity, these structures are denoted by their masses. For the species having the same mass, they are numbered by A, B,... The characteristics of these molecules, including equilibrium geometries, total energies, and vibrational wavenumbers will be given in a separate article.<sup>25</sup>

In addition to the [TVS<sup>+</sup>], trivinylsilane<sup>+</sup>, divinylsilane<sup>+</sup>, vinylsilane<sup>+</sup>, and vinyl radical, we are computing forms containing aromatic cycles (e.g., [DMPS<sup>+</sup>] for dimethylphenylsilane cation, the [121E<sup>+</sup>] species,...), others with alkyne branches (e.g., [121C<sup>+</sup>], [79C],...), and some heterocyclic forms (e.g., [121D<sup>+</sup>], [108C<sup>+</sup>],...) together with saturated and unsatur-

ated organic compounds. The analysis of these data shows the diversity of the molecular species that can be formed after TVS<sup>+</sup> formation under these experimental conditions. Mainly, our calculations reveal that two classes of processes can occur: (1) isomerization and (2) fragmentation. This is not surprising for silicon-containing organic molecules as pointed out in the Introduction.<sup>1-3</sup> Let us consider, for instance, that at the parent peak at 136, a second form is found. It is denoted as DMPS<sup>+</sup>, for which a neutral species exists. Our MP2/cc-pVDZ vertical ionization energy for DMPS is computed to be  $\sim 8.91$  eV, which is in close accord with the experimental value of  $8.92 \pm 0.15$  eV of Gaidis et al.<sup>26</sup> Again, this validates the good accuracy of these computations.

#### IV. Discussion

In this section, we present our tentative assignment of the experimental data according to ab initio calculations. As can be seen, for a measured ion with given  $m/z$  several possible structures can be found. We try to identify possible structures on the basis of calculated AE values, which we compare with experimental AE values. In the present experiment, we were not able to measure the kinetic energy release of the fragment ions that would allow us to identify the products more precisely. Therefore, we list all ions that could be formed at and above the experimental appearance energy. We give also the trivial dissociation limits (Si-C bonds breakings from TVS<sup>+</sup>) even if they are not energetically accessible.

- Peak at 136. We calculated two possible structures: the parent TVS<sup>+</sup> as discussed above and DMPS<sup>+</sup> with calculated AE of 5.7 eV. We also calculated a third structure, denoted [136<sup>+</sup>] (cf. Figure 3 for more details). The electron impact ionization is a vertical process, and thus formation of the parent molecular ion TVS<sup>+</sup> is the initiating process. The experimental AE of  $9.5 \pm 0.12$  eV is in very good agreement with the calculated one (9.45 eV). The TVS<sup>+</sup>, however, may undergo rearrangement into other [136<sup>+</sup>] or DMPS<sup>+</sup>, which may then further dissociate.
- Peak at 121. The experimental AE of the ionic species associated with  $m/z$  of 121 has a value of  $10.1 \pm 0.12$  eV. We calculated five exit channels: [121A<sup>+</sup>] + CH<sub>3</sub>, [121B<sup>+</sup>] + CH<sub>3</sub>, [121C<sup>+</sup>] + CH<sub>3</sub>, [121D<sup>+</sup>] + CH<sub>3</sub>, and [121E<sup>+</sup>] + CH<sub>3</sub> (Table 1) with the following AEs: 16.5, 10.7, 9.2, 7.9, and 6.8 eV, respectively. The appearance energy of the [121A<sup>+</sup>] is above the experimental one, and thus this ion is not formed there. However, the four other channels cannot be excluded, and they are expected to constitute this mass peak. It is worth noting that the [121E<sup>+</sup>] ion could be formed as a product of the isomerization of TVS<sup>+</sup> into DMPS<sup>+</sup> and subsequent dissociation of the methyl group. The mass spectrum of DMPS available in the NIST database shows that the most intense peak is with  $m/z$  of 121 and probably corresponds to this [121E<sup>+</sup>] ion.
- Peak at 109. The mass difference between this peak and TVS<sup>+</sup> indicates that it is formed via the dissociation of a vinyl group from the TVS<sup>+</sup>. The calculated value of the appearance energy supports this assignment.
- Peak at 108. This ion belongs to the most important peaks in the mass spectrum. As the mass of the ion indicates, ethylene is most probably formed in this reaction channel. We investigated theoretically four possible organosilicon ions in connection with ethylene formation. We calculated AEs in the 7.8–11.1 eV range. The threshold for [108A<sup>+</sup>] formation is computed at 11.1 eV, and thus this channel is not accessible at the experimental threshold of  $9.4 \pm 0.12$  eV. However,

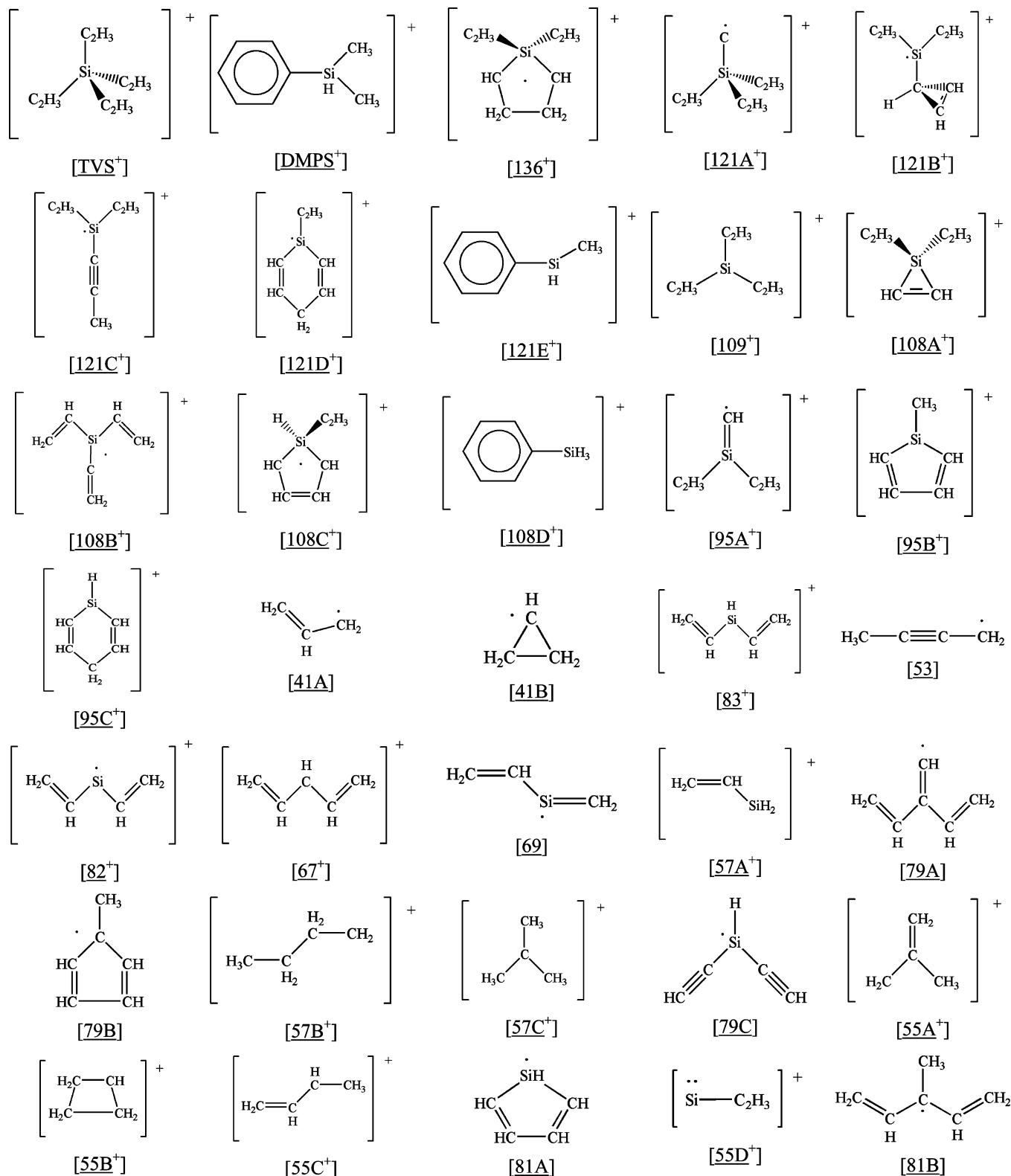


**Figure 3.** Calculated ionic and neutral structures and their designation.

reasonable good agreement is found for  $[108B^+]$  + ethylene and  $[108C^+]$  + ethylene. The reaction  $[108C^+]$  + ethylene indicates that rearrangement reaction  $[TVS^+] \rightarrow [136^+]$  followed by dissociation processes could be operative.

- Peak at 95. Six possible structures were studied. They are given in Table 1. All of them lead to the formation of an ionic organosilicon molecule together with either the allyl radical  $[41A]$  or the cyclopropyl radical  $[41B]$ . The  $[95A^+]$

+  $[41A]$  and  $[95A^+]$  +  $[41B]$  channels are out of the range of the accessible energies here, whereas we expect the occurrence of the four others.

- Peak at 83. This is the most intense peak in the mass spectrum. It corresponds to the formation of protonated divinylsilane (i.e.,  $[83^+]$  structure of Figure 3). The neutral species formed are either  $C_2H_3 + C_2H_2$  or but-2-yn-1-yl radical  $[53]$ . The experimental AE of 9.8 eV indicated that at the threshold

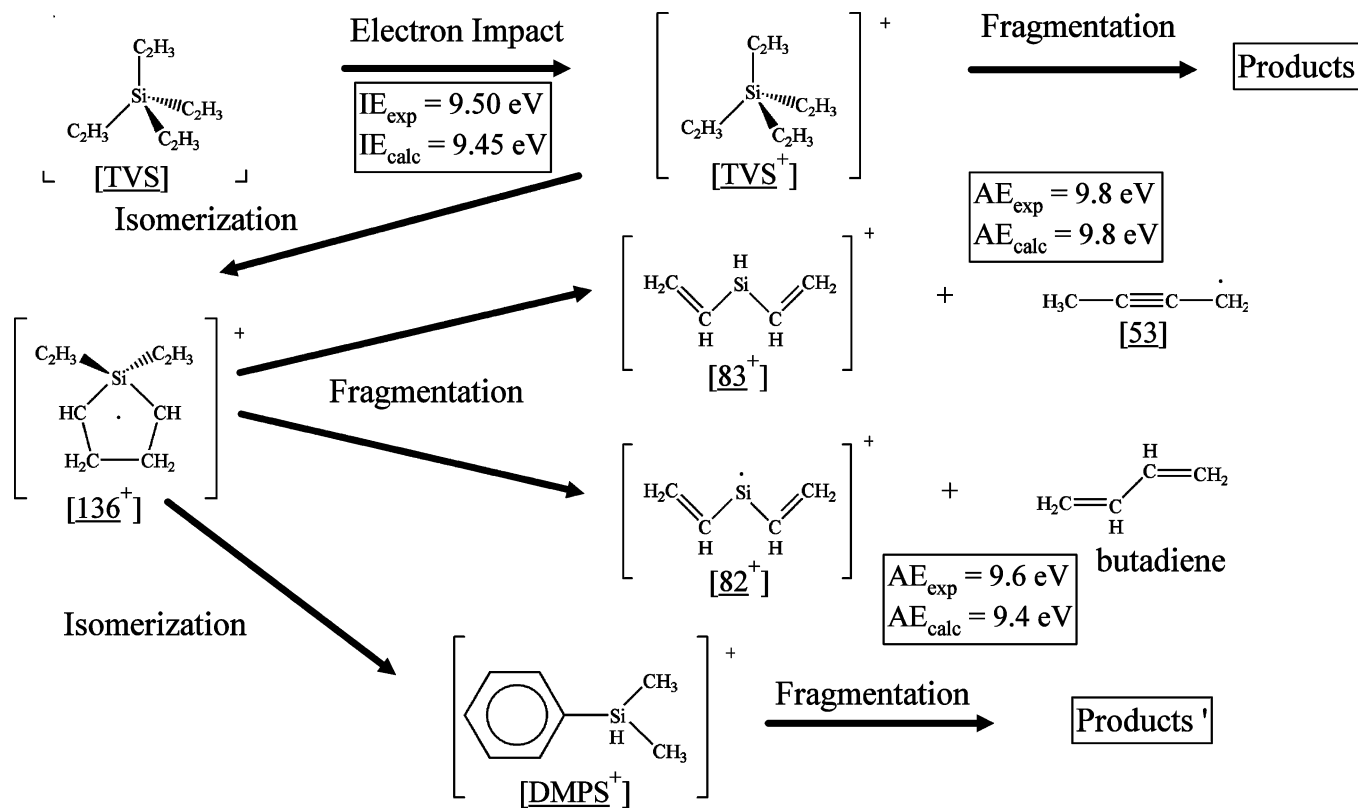


**Figure 4.** Summary of the processes occurring after ionization of TVS by electron impact.

[83<sup>+</sup>] + [53] channel is open. Present calculations show that this reaction channel with calculated AE of 9.8 eV is accessible through formation of [136<sup>+</sup>] ion from TVS<sup>+</sup> and its decomposition.

- Peak at 82. The removal of two vinyls from TVS<sup>+</sup> leads to a dissociation limit located at 14.8 eV, which is energetically higher than the experimental AE of 9.6 eV. However, the formation of butadiene and divinylsilane ([82<sup>+</sup>]) represents a reasonable alternative with computed AE of 9.4 eV. One important question is: How is butadiene formed in a gas-phase unimolecular reaction? A possible explanation is the following: TVS<sup>+</sup> isomerizes first into [136<sup>+</sup>], then H-transpositions between the carbons of the five-membered ring take place, followed by sigmatropic reactions.
- Peak at 67. The unique decomposition products close to the measured AE are the 1,4-pentadiene cation [67<sup>+</sup>] + ylide carbon of vinylsilane radical [69]. [69] is of particular interest for organic and astrochemistry of circumstellar shells, where 10% of the discovered molecules contain silicon.<sup>6,7</sup>
- Peak at 57. A priori, the [57A<sup>+</sup>] + [79B] and [57C<sup>+</sup>] + [79C] channels are open. Both of them are expected to contribute to our mass spectrum.
- Peak at 55. Similar to a previous case, we suggest several products for this peak. Readers are referred to Figure 3 and Table 1 for more details. Especially, our computed AE for [55D<sup>+</sup>] + C<sub>4</sub>H<sub>6</sub> + C<sub>2</sub>H<sub>3</sub> coincides with the 12.3 eV threshold determined presently. This channel is of particular importance since the corresponding products are solely formed through the decomposition of [136<sup>+</sup>].
- Peaks at 43, 31, and 29. We give in Table 1 the ionic species that correspond to these masses. A huge amount of neutral molecules are associated with these cations. For more clarity of the article, we do not depict all possibilities here.

In the present experiment, the time delay between ion creation and its detection is in the range 20–60 μs. This time scale is

sufficient for the ion rearrangement. Figure 4 summarizes the mechanism of the chemistry of TVS<sup>+</sup> formed by electron impact ionization of TVS. The initial step is the formation of the TVS<sup>+</sup> ion that can directly dissociate or may rearrange into [136<sup>+</sup>] ion, which may further dissociate into more stable products. Over a long time, isomerization of the tetravinylsilane cation into dimethylphenylsilane cation is expected in competition with the fragmentation processes.

## V. Conclusions

We present a combined theoretical and experimental work on the reactivity of tetravinylsilane cation formed after electron impact. The mass spectrum and the appearance energies of the products were analyzed and assigned by means of ab initio calculations. This work should motivate new experiments on the photoionization of TVS and more generally of organosilicon compounds, such as zero kinetic energy electron techniques together with coincidence methods (e.g., threshold photoelectron photoion coincidence or pulsed field ionization photoelectron photoion) to perform state-to-state unimolecular decomposition of TVS<sup>+</sup>. This allows determining the kinetic energy releases associated with each ionic fragment for their identification.

In addition, our calculations reveal the formation of new organosilicon molecules either neutral or ionized, which can be possible chemical intermediates or final products in Si-containing media relevant for astrochemistry, plasma, and organic chemistry.

**Acknowledgment.** This work was supported by European project PHC (Barrande France–Czech Republic, under Contract No. 13885PJ 2007–2008), Slovak Science and Technology Assistance Agency (under Contract No. APVV-0365-07), and the European Commission. F.K. thanks the Czech Ministry of Education for financial support (Research Plan No. 0021630501).

## References and Notes

- (1) Raabe, G.; Michl, J. *Chem. Rev.* **1985**, *85*, 419.
- (2) Apeloig, Y.; Karni, M.; Stanger, A.; Schwartz, H.; Drewello, T.; Czekay, G. *J. Chem. Soc., Chem. Commun.* **1987**, 989, and references therein.
- (3) Magnera, T. F.; Balaji, V.; Michl, J.; Miller, R. D.; Sooriyakumaran, R. *Macromolecules* **1989**, *22*, 1624.
- (4) Igawa, K.; Takada, J.; Shimono, T.; Tomooka, K. *J. Am. Chem. Soc.* **2008**, *130*, 16132.
- (5) Denmark, S. E.; Butler, C. R. *J. Am. Chem. Soc.* **2008**, *130*, 3690.
- (6) McCarthy, M. C.; Gottlieb, C. A.; Thaddeus, P. *Mol. Phys.* **2003**, *101*, 697.
- (7) Cernicharo, J.; Gottlieb, C. A.; Guélin, M.; Thaddeus, P.; Vrtilek, J. M. *Astrophys. J. Lett.* **1989**, *341*, L25.
- (8) Fonseca, J. L. C.; Badyal, J. P. S. *Macromolecules* **1992**, *25*, 4730.
- (9) Fonseca, J. L. C.; Tasker, S.; Apperley, D. C.; Badyal, J. P. S. *Macromolecules* **1996**, *29*, 1705.
- (10) Davidson, G. *Spectrochim. Acta* **1971**, *27A*, 1161, and references therein.
- (11) Rustad, S.; Beagley, B. *J. Mol. Struct.* **1978**, *48*, 381, and references therein.
- (12) Pola, J.; Parsons, J. P.; Taylor, R. *J. Organomet. Chem.* **1995**, *489*, C9.
- (13) Drinek, V.; Bastl, Z.; Subrt, J.; Taylor, R.; Pola, J. *J. Anal. Appl. Pyrolysis* **1995**, *35*, 199.
- (14) Schweig, A.; Weidner, U.; Berger, J. G.; Grahn, W. *Tetrahedron Lett.* **1973**, *8*, 557.
- (15) Cech, V.; Studynka, J.; Conte, N.; Perina, V. *Surf. Coat. Technol.* **2007**, *201*, 5512.
- (16) Studynka, J.; Cechalova, B.; Cech, V. *Surf. Coat. Technol.* **2008**, *202*, 5505.
- (17) Rašková, Z. *Plasma Diagnostics during Thin Films Depositions*; Vutium: Brno, Czech Republic, 2006.
- (18) Stano, M.; Matejcik, S.; Skalny, J. D.; Märk, T. D. *J. Phys. B: At., Mol. Opt. Phys.* **2003**, *36*, 261.
- (19) NIST Chemistry WebBook. <http://webbook.nist.gov>.
- (20) Dunning, T. H., Jr. *J. Chem. Phys.* **1989**, *90*, 1007.
- (21) Woon, D. E.; Dunning, T. H., Jr. *J. Chem. Phys.* **1993**, *98*, 1358.
- (22) Hampel, C.; Peterson, K.; Werner, H.-J. *Chem. Phys. Lett.* **1992**, *190*, 1, and references therein.
- (23) Amos, R. D.; Andrews, J. S.; Handy, N. C.; Knowles, P. J. *Chem. Phys. Lett.* **1991**, *185*, 256.
- (24) Werner, H.-J.; Knowles, P. J.; Lindh, R.; Manby, F. R.; Schütz, M.; Celani, P.; Korona, T.; Mitrushenkov, A.; Rauhut, G.; Adler, T. B.; Amos, R. D.; Bernhardsson, A.; Berning, A.; Cooper, D. L.; Deegan, M. J. O.; Dobbyn, A. J.; Eckert, F.; Goll, E.; Hampel, C.; Hetzer, G.; Hrenar, T.; Knizia, G.; Köppl, C.; Liu, Y.; Lloyd, A. W.; Mata, R. A.; May, A. J.; McNicholas, S. J.; Meyer, W.; Mura, M. E.; Nicklass, A.; Palmieri, P.; Pflüger, K.; Pitzer, R.; Reiher, M.; Schumann, U.; Stoll, H.; Stone, A. J.; Tarroni, R.; Thorsteinsson, T.; Wang, M.; Wolf, A. Molpro Quantum Chemistry Package. <http://www.molpro.net>.
- (25) Manuscript in preparation.
- (26) Gaidis, J. M.; Briggs, P. R.; Shannon, T. W. *J. Phys. Chem.* **1071**, *75*, 974.

JP901978J